Project Number: SW0107

Failure Methods, Clamp Load, and Heat in Self-Tapping Screw Insertion

A Major Qualifying Project Report

submitted to the Faculty

of the

WORCESTER POLYTECHNIC INSTITUTE

in partial fulfillment of the requirements for the

Degree of Bachelor of Science

by

Jonathan D. Adler

Date: August 20, 2007

Approved:

Professor Suzanne L. Weekes, Advisor

1. Screw
2. Failure
3. Heat

Abstract

A self-tapping screw is a high-strength one-piece fastener that is driven into preformed holes. The goal of the Major Qualifying Project (MQP) completed by A. Leo et al. [5] and the Research Experience for Undergraduates (REU) completed by Miller et al. [4] was to create a mathematical model that allows users to input data about their self-tapping screw and the material it is entering and would output a torque curve which models the fastening process. We improve the algorithm to include the modeling of the failure of the joint as well as a model for the clamp load of the joint. We also investigate a model of heat generation in the screw that includes the speed of screw insertion.

Acknowledgments

I would like to thank Professor Suzanne Weekes for her guidance on this project and her willingness to discuss it no matter the time nor the place. I would also like to thank Craig Adamson and the BOSE Corporation for providing me with this project and for allowing me to use BOSE equipment. I would like to thank Angela Leo, Sanjayan Manivannan, Jason Miller, John Potter, Alla Shved, and Lingfeng Tang for their previous work on this topic for without it this project would never be possible. Finally I would like to thank Professor Arthur Heinricher, Professor Jayson Wilbur, and the WPI Center for Industrial Mathematics and Statistics for their assistance in my undergraduate research experience.

Contents

Chapter 1

Introduction

This paper contains research done by the NSF-supported 2006 REU program in Industrial Mathematics and Statistics at WPI. Sections 1, 2.1, 2.2, 2.3, and 2.4 were mostly researched and written by the 2006 group while sections 2.5, 3, and 4 were done for this MQP which was also part of the 2007 REU program. All other sections have writing done by both groups.

A self-tapping screw is a high-strength one-piece fastener that is driven into preformed holes. As the screw is driven into the material, it forms its own mating threads. As a result, there is a very good thread fit which enhances resistance to thread loosening. Self-tapping screws are commonly used for fastening in assembly operations. Their use not only simplifies the fastening process but also results in lower production costs. Materials joined together with screws can be easily disassembled, whether it be for repair or maintenance, and then reassembled. Furthermore, screws can be used to vary the compressive force with which materials are held together.

BOSE Corporation is a company that makes high-quality audio equipment. They use automated machines to assemble their products with self-tapping screws. During this process, however, they may experience material failure in the form of breaking of the screw just below the screw head and stripping of the formed threads in the product material if the torque used for screw insertion is set too high.

The goal of the Major Qualifying Project (MQP) completed by A. Leo, et al. [5] was to analyze and improve a mathematical model of the self-tapping screw insertion process found in [8] so that it could be used in manufacturing processes at the BOSE Corporation. A Graphical User Interface (GUI) was built in MATLAB® to provide a user-friendly method of generating a torque curve for any set of materials with various properties. The authors of [5] collected experimental data at BOSE and compared it with the theoretical results from the model. Though there was fairly good agreement between the model and experimental data, there were some noticable differences. Possible reasons for these discrepancies were presented in [5], and included the heat generated by friction.

The goal of this project is to refine the model in [5] by calculating maximum allowable tightening torque before material failure, and by relaxing the assumption that heat generated by friction is negligible. We predict that factoring in heat will help to better fit the torque curve to the actual data as well as better predict the maximum allowable torque before tightening.

1.1 Assumptions

In order to create a model of the screw insertion process, assumptions are made to simplify the system. The following is an itemized list of assumptions as is found in [5].

- The holes in the near plate and top of the tap plate are perfectly aligned with each other.
- The screw is centrally positioned and the axis is correctly aligned with the holes.
- The screw is rigidly coupled to the driver and only moves along and about the screw axis.
- The tightening speeds are sufficiently low for the inertia forces to be negligible.
- The plate material is isotropic and homogeneous.
- The near plate has a hole with a diameter greater than the screw major diameter and a flat surface plane normal to the hole central axis.
- The tap plate has a clean hole with a diameter greater than or equal to the root diameter of the screw and less than the major diameter of the screw.
- The driver applies just sufficient axial force and torque to allow the screw to advance.
- A balanced axial force is applied during screw fastening.
- The finishing coat used on the screw is not considered a part of the system.
- The screw tapers uniformly from the leading end so that the full thread cross-sectional area rate of change with respect to the helix angular position is constant throughout the tapered part, and at the tip of the screw the thread cross-sectional area is zero.
- The cutting portion of the tapered region of the screw is shorter than the depth of the hole in the tap plate.
- The thread helix angle θ is constant along the entire screw.
- Engagement ends before the untapered portion of the screw comes into contact with the tap plate.

In the model presented in [5], they took into account a tap hole with a draft angle $\lambda > 0$ and asymmetric threads. We assume that there is no draft angle in the tap hole and for calculating the failure torque we assume that the threads are symmetric.

1.2 Screw Geometry

Figure 1.1 is a diagram of a self-tapping screw with the significant parameters labeled. The picture shows the screw just before the insertion process begins, where the tapered portion of the screw has just made contact with the tap plate. We define the angular rotation ϕ at this point to be zero. The tap plate is the object into which the tapered portion of the screw will tap threads. The diameter of the tap hole at the top of the tap plate D_{h0} is constant along the hole, and we define this as D_h. The parameters β_1 and β_2 represent the lead and trail angles of the thread. When we assume that the threads are symmetric, $\beta_1 = \beta_2 = \beta$, which we define as the thread crest half-angle. The point $\phi = \alpha$ is also labeled, and is the point at which the untapered region of the screw begins. The value α corresponds to the rotation necessary to first make the untapered portion of the screw come in contact with the tap plate. The helix angle θ is the angle that the crest of the screw thread makes with the horizontal. The root diameter D_r is the diameter of the screw without the threads, and the major diameter D_s is the diameter of the screw including the threads. The near plate has a

hole with diameter D_n, and this diameter must be greater than D_s (see assumptions). In order for the screw to effectively fasten the near and tap plates together, the screw head diameter D_{sh} must be larger than D_n. The pitch p is the distance between two consecutive crests of the screw threads. D_p is the pitch diameter which is the distance between the threads where the width of the threads are equal. In a screw with symmetric threads, $D_p = \frac{D_s+D_r}{2}$.

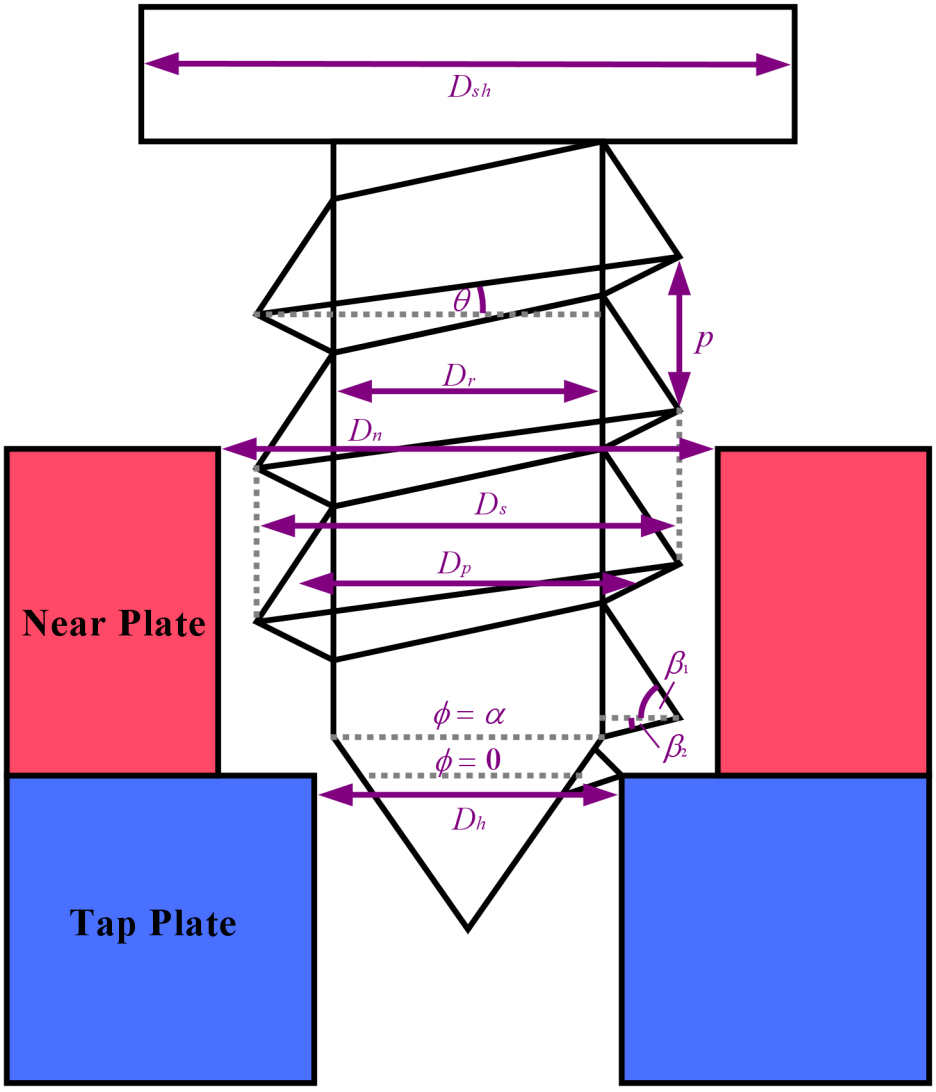

Figure 1.1: Screw Geometry

1.2.1 Parameterization of Screw

Consider a point at position (x, y, z) on the screw where the central axis of the screw corresponds to the z-axis and $z = 0$ is aligned with the top of the tap plate when the screw is just placed into the tap plate hole. Let r be the distance from the screw central axis to the point. In terms of the thread helix angle θ and the helix coordinate variable ϕ, this point has coordinates

$$\begin{aligned} x &= r\cos(\phi) \\ y &= r\sin(\phi) \\ z &= r\tan(\theta)(\phi). \end{aligned}$$

Here, $\phi = 0$ corresponds to the helical coordinate for which the major diameter of the tapered region of the screw is equal to D_h; that is, the first position of the screw that makes contact with the tap plate upon insertion. The untapered length of the screw begins at $\phi = \alpha$. See Figure 1.1.

1.2.2 Phases of Insertion

The process of screw insertion has four phases characterized by the portion of the screw engaged in the tap plate material. The value of ϕ at the top of the tap plate is referred to as $\bar{\phi}$; this is also the amount of rotations that the screw has undergone during insertion. The first $\overline{\phi}$ range begins at the first point of contact between the screw and the tap hole, $\bar{\phi} = 0$, and ends when the top of the tapered portion of the screw, $\overline{\phi} = \alpha$, comes into contact with the top of the tap plate. This is shown in Figure 1.2. The second range concludes when the lowest point of cutting on the screw has just broken through the bottom of the tap plate, denoted by $\overline{\phi} = \phi_b$. This is illustrated in Figure 1.3. The third $\overline{\phi}$ range ends when the top of the tapered portion of the screw has broken through the tap plate; this is also when cutting ends completely. See Figure 1.4. The final range for $\overline{\phi}$ is when there is strict advancement, and it occurs for $\overline{\phi} > \phi_b + \alpha$ and goes until seating when $\overline{\phi} = \phi_t$ as shown in Figure 1.5.

The different phases of insertion are important because the torque calculated in [5] was over these phases, and each phase has a different torque. Therefore, when incorporating heat into the torque equations, we must take into account these intervals.

1.2.3 Torque Curve

A *torque curve* is a graph of rotation of a screw $\bar{\phi}$ versus the torque required to continue the insertion process; see Figure 1.6. By analyzing a torque curve, information about screw insertion can be found. Automatic screwdrivers work by having a torque ceiling such that, when inserting the screw, if that amount of torque is ever applied the machine will stop turning the screw. The drive torque T_{drive} is the minimum amount of torque required to seat the screw. The fail torque T_{fail} is the minimum amount of torque which, when applied to the screw, will cause the joint to fail. So for screw insertion BOSE needs to find a torque ceiling to input into the automatic screwdriver that is greater than the drive torque to ensure seating put less than the fail torque to avoid compromising the joint.

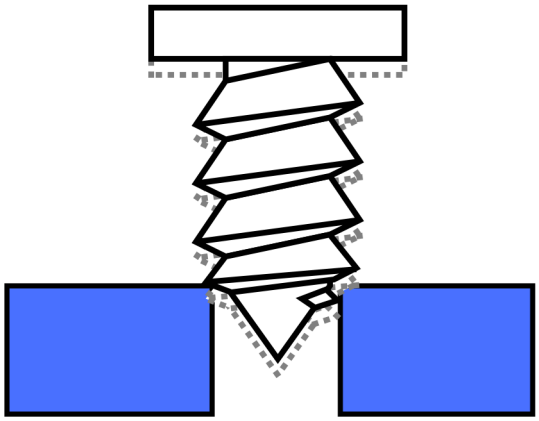

Figure 1.2: $0 \leq \bar{\phi} \leq \alpha$

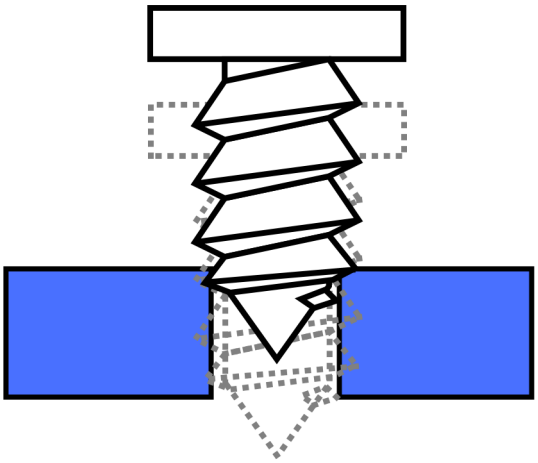

Figure 1.3: $\alpha \leq \bar{\phi} \leq \phi_b$

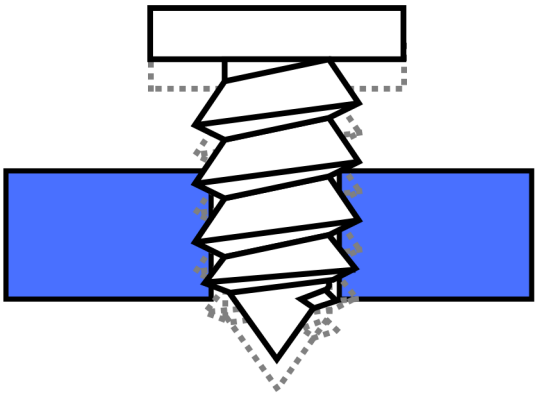

Figure 1.4: $\phi_b \leq \bar{\phi} \leq \phi_b + \alpha$

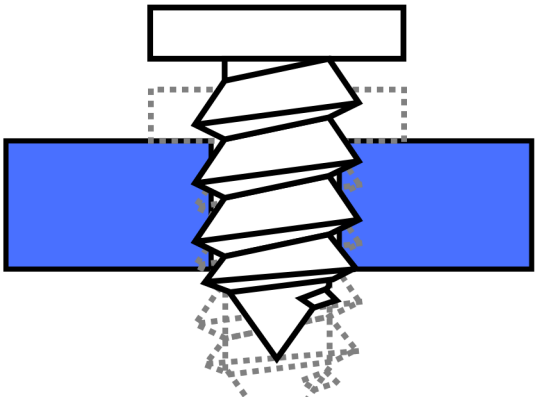

Figure 1.5: $\phi_b + \alpha \leq \bar{\phi} \leq \phi_t$

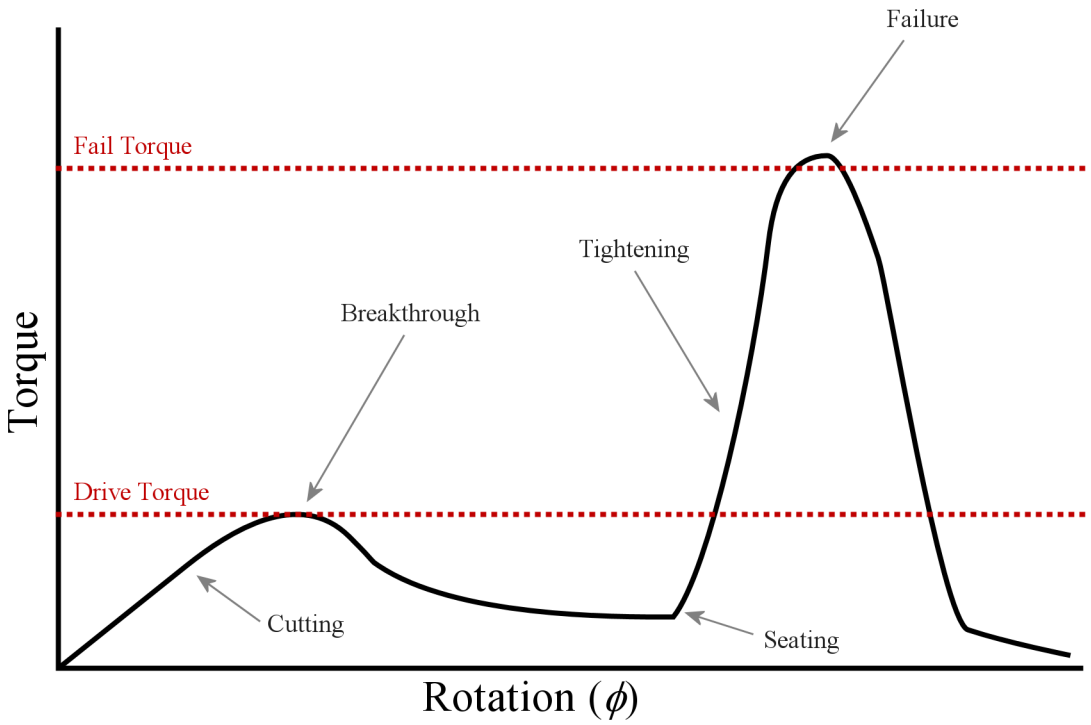

Figure 1.6: A sample torque curve

Chapter 2

Screw Failure During Tightening

The tightening process begins when the lower surface of the screw head makes contact with the near plate material. This occurs when $\overline{\phi} = \phi_t$. At this point and beyond, all of the applied torque, or rotational force, goes into overcoming the internal stress of the materials as well as friction forces on the head of the screw. As the screw is tightened, the internal stresses increase. However, certain stresses may cause failure if the torque is too high. The model presented in [5] calculates the torque required to advance a screw a small amount after it is seated, but does not investigate failure that may occur during tightening.

2.1 Failure Modes in Tightening

Tightening gives rise to various stresses in the screw and material. The stress σ on a region of area A is given by $\sigma = P/A$ where P is the load acting on the region. The tightening process can be broken down into three distinct stages. In the first stage of tightening, the stresses cause elastic deformation of the joint materials; that is if the screw is removed there would be no permanent deformation of the screw or plate. The next stage, the plastic region, is where permanent deformation occurs. This deformation happens when one of the stress levels of the screw or material reaches its respective yield strength. At this point, if the screw were to be removed it would not return to its original state. Once we exceed the yield strength of a material, we enter the final stage where breaking will occur. Breaking occurs when the ultimate strength of the material is achieved. Although the joint still will work once the ultimate yield strength is passed, it will not be as strong, so we consider failure to occur when the yield strength is reached.

For our model we consider three types of failure modes that might occur during tightening: stripping failure in the tap plate material, bearing failure in the near plate material, and breaking of the screw. Stripping is when the force between the screw thread and plate material is so great that the plate material breaks. At this point there is nothing holding the screw in the tap plate because the threads of the screw have sheared off the formed threads in the material. After stripping, if we were to remove the screw from the tap hole we would observe the failed material filling in the volume between the screw threads. Bearing failure is permanent deformation of the near plate due to the compressive force of the screw head. Breaking of the screw is when the screw snaps due to the applied forces during tightening.

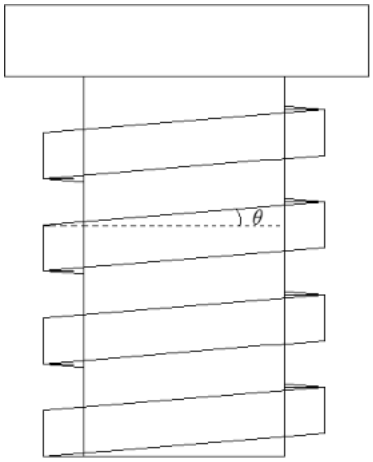

Figure 2.1: Power screw with square threads ($\beta = 0$)

2.2 Torque Required to Overcome Internal Stress

To find the torque to cause the different types of failure we must first understand how the applied torque creates internal forces in the joint. Once we have found this relationship we can find the forces to cause failure, and then relate applied torque to failure. To find the relationship between torque and internal force, we will first consider the simple case of a screw with square threads ($\beta = 0$) and then in Section 2.2.2 we will extend this to self-tapping screws with symmetric threads ($\beta_1 = \beta_2 = \beta > 0$).

2.2.1 Two-Dimensional Model

First we will look at a simplified analogy of a screw during the tightening process. In the next section we will extend it to parameters that are better suited for our purpose.

The process of tightening the screw is analogous to a power screw lifting a mass. An example of a power screw is a basic car jack which is used to lift a vehicle off the ground for maintenance and repair. During insertion, one may take the point of view that the screw is immobile and the material is moving counter clockwise up the thread. When making this comparison, it is important to note the differences between a power screw and self-tapping screw. A power screw uses square threads ($\beta = 0$, shown in Figure 2.1) to convert applied torque into linear motion. In addition, a power screw lifts a load that is just the weight of an object, while the load for a self-tapping screw during tightening is the load corresponding to stresses of the materials.

Since a power screw uses square threads, all of the forces can be broken down into x (azimuthal) and z (axial) components; we essentially have a two-dimensional problem. Consider Figure 2.2. The inclined plane represents a thread that has been unwrapped from the screw, while the rectangle on the inclined plane represents a mass of plate material on the screw thread. This mass creates a load P that acts downward on the screw threads. The normal force N, perpendicular to the surface, is the force of the threads pushing on the mass. The frictional force which opposes the intended movement, is $\mu_1 N$ where μ_1 is the coefficient of friction between the screw and plate material. The force F is caused by the torque applied to the screw. There is no acceleration, so the net force is zero, and therefore $F_x = 0$ and $F_z = 0$, where F_x and F_z are the horizontal (actually, azimuthal) and vertical components of the net force, respectively. This leads to the

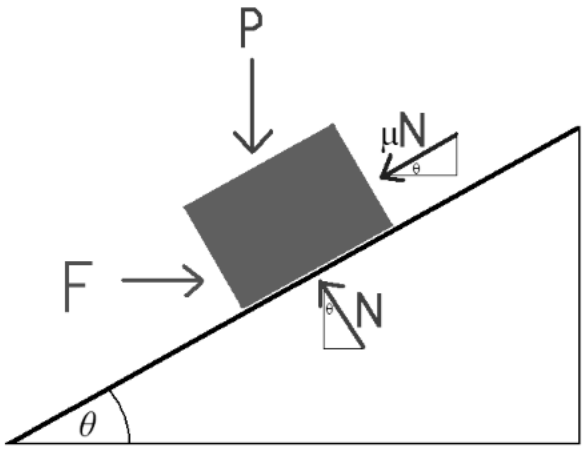

P - load from tap plate threads
F - force from applied torque
N - normal force
μN - friction force

Figure 2.2: Unwrapped thread section with labeled forces

following [6]:

$$F_x = F - \mu_1 N\cos\theta - N\sin\theta = 0 \tag{2.1}$$

$$F_z = N\cos\theta - \mu_1 N\sin\theta - P = 0 \tag{2.2}$$

Solving for F, we get

$$F = P\frac{\mu_1\cos\theta + \sin\theta}{\cos\theta - \mu_1\sin\theta}. \tag{2.3}$$

The magnitude of torque T_1 required to exert a force of magnitude F is the force times the radius at which it acts. Thus

$$T_1 = P\frac{\mu_1\cos\theta + \sin\theta}{\cos\theta - \mu_1\sin\theta}\left(\frac{D_s + D_h}{4}\right) \tag{2.4}$$

where D_s is the screw major diameter and D_h is the tap hole diameter.

2.2.2 Three-Dimensional Model

Consider a self-tapping screw. A self-tapping screw uses non-square threads $\beta > 0$ to convert applied torque into a clamp load force. This results in a snug fit between the near plate and tap plate, with a nonzero thread-crest half-angle β. There is a third component that must be taken into account when finding the normal force N. This is essentially a perpendicular cross-section of Figure 2.2 but with $\beta > 0$. See Figure 2.3. The material still only moves in the x-z direction so P, F and $\mu_1 N$ remain as in Figure 2.2. However, as illustrated in Figure 2.3, the normal force now has a radial component. We project the normal force onto the

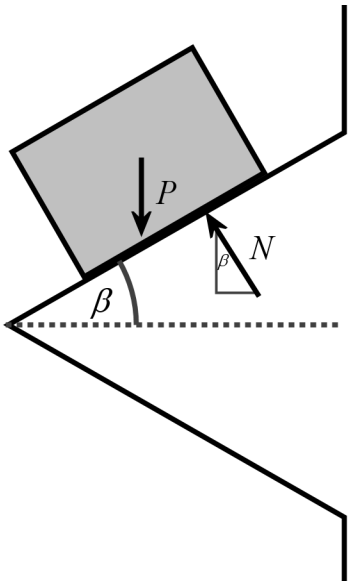

Figure 2.3: Cross-section of thread showing the effect of β.

x-z plane by multiplying it by $\cos\beta$. This leads to the following:

$$F_x = F - \mu_1 N\cos\theta - N\sin\theta\cos\beta = 0 \tag{2.5}$$

$$F_z = N\cos\theta\cos\beta - \mu_1 N\sin\theta - P = 0 \tag{2.6}$$

Again substituting in for N and solving for F, we get

$$F = P\frac{\mu_1\cos\theta + \sin\theta\cos\beta}{\cos\theta\cos\beta - \mu_1\sin\theta}. \tag{2.7}$$

The torque T_1 required to exert this force is

$$T_1 = P\frac{\mu_1\cos\theta + \sin\theta\cos\beta}{\cos\theta\cos\beta - \mu_1\sin\theta}\left(\frac{D_s + D_h}{4}\right). \tag{2.8}$$

The effective load P is the force on the threads related to internal stresses of the material as discussed in Section 2.1.

2.2.3 Torque Required to Overcome Screw Head Friction

When the screw head comes into contact with the near plate, i.e. seats, and continues to rotate, there is friction between the bottom of the screw head and the top of the near plate. This friction force opposes the direction of motion and has a magnitude equal to the normal force times the coefficient of friction between the two materials. The torque T_2 required to overcome friction is the product of the frictional force and the average radius at which the friction force is acting,

$$T_2 = \mu_2 P\left(\frac{D_{sh} + D_n}{4}\right). \tag{2.9}$$

Here D_{sh} is the screw head diameter, D_n is the near hole diameter, P is the load exerted on near plate, and μ_2 is the coefficient of friction of the head of the screw touching the near plate; see Figure 2.4.

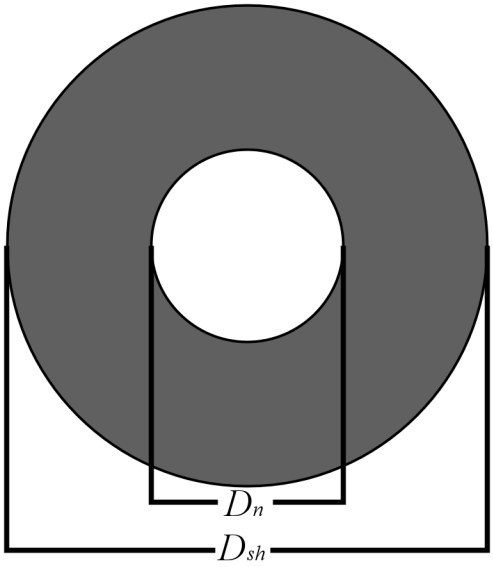

Figure 2.4: Diagram of contact between screw head and near plate.

2.2.4 Total Tightening Torque

The total torque T required to overcome the forces occurring during the tightening process is the sum of the individual torques. It is the sum of the torques to overcome all the internal stresses (2.8) and friction (2.9),

$$T = P\left(\frac{\mu_1 \cos\theta + \sin\theta\cos\beta}{\cos\theta\cos\beta - \mu_1\sin\theta}\left(\frac{D_s + D_h}{4}\right) + \mu_2\left(\frac{D_{sh} + D_n}{4}\right)\right). \tag{2.10}$$

2.3 Failure Due to Stripping

Stripping of the tap plate material is due to a shear stress. Shear stress is the stress that occurs at an area due to a perpendicular or tangential force acting on that area. When the engaged threads can no longer advance downwards, the torque applied to the screw creates an upward force on the threads of the tap plate material. This force P_s produces a shear stress along the surface of a vertical cylinder with diameter D_s in the tap plate. The magnitude of the shear stress caused by a downward load P_s acting on a surface area A_s is

$$\tau_s = \frac{P_s}{A_s}.$$

If τ_s exceeds the shear yield strength of the tap plate material, τ_{yt}, stripping of the material will occur at the major diameter of the screw. The surface area A_s, shown in Figure 2.5, is

$$A_s = \pi D_s n_t p,$$

where D_s is the major diameter of the screw, n_t is the number of engaged threads, and p is the pitch. The shear stress in the tap plate material is

$$\tau_s = \frac{P_s}{\pi D_s n_t p}.$$

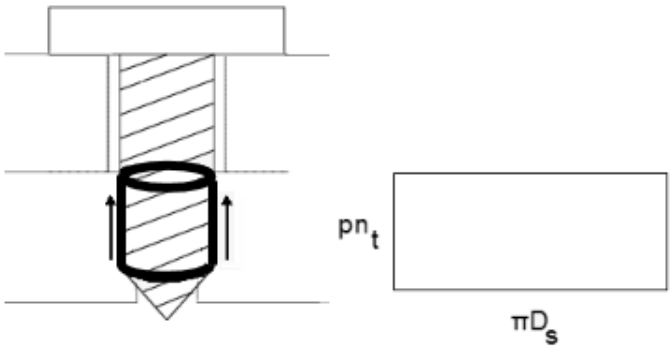

Figure 2.5: Area of Shear Stress.

Thus stripping occurs when the load is equal to $\tau_{yt} D_s n_t p \pi$. We can use this and (2.10) to find the torque required to cause failure by stripping

$$T_{stripping} = \tau_{yt} D_s n_t p \pi \left(\frac{\mu_1 \cos\theta + \sin\theta \cos\beta}{\cos\theta \cos\beta - \mu_1 \sin\theta} \left(\frac{D_s + D_h}{4} \right) + \mu_2 \left(\frac{D_{sh} + D_n}{4} \right) \right), \tag{2.11}$$

if the only internal stress to overcome were the shear stress of the tap plate material.

2.4 Bearing Failure

When the head of the screw is seated on the near plate, the downward force that occurs due to tightening creates a compressive stress on the plate, known as bearing stress. The bearing stress that the plate material experiences is:

$$\sigma_b = \frac{P_b}{A_b},$$

where P_b is a downward force that occurs due to tightening and the area under compression is the contact surface of the near plate and screw head. Shown in Figure 2.4, this contact surface is an annulus with outer diameter equal to the screw head diameter D_{sh} and inner diameter equal to the near hole diameter D_n so that

$$A_b = \pi \frac{D_{sh}^2 - D_n^2}{4}.$$

Combining those two equations gives us the bearing stress

$$\sigma_b = \frac{4P}{\pi (D_{sh}^2 - D_n^2)}.$$

If the bearing stress exceeds the yield strength of the near plate material, the near plate would be permanently deformed in the shape of the annulus with area equivalent to A_b. Bearing failure occurs when the load is equal to $\sigma_{yn} \left(\frac{\pi (D_{sh}^2 - D_n^2)}{4} \right)$ where σ_{yn} is the yield strength of the near plate. So, if all the torque applied goes into overcoming bearing stress only, the minimum torque to cause bearing failure (2.10) is would be

$$T_{bearing} = \sigma_{yn} \left(\frac{\pi (D_{sh}^2 - D_n^2)}{4} \right) \left(\frac{\mu_1 \cos\theta + \sin\theta \cos\beta}{\cos\theta \cos\beta - \mu_1 \sin\theta} \left(\frac{D_s + D_h}{4} \right) + \mu_2 \left(\frac{D_{sh} + D_n}{4} \right) \right). \tag{2.12}$$

2.5 Screw Fracture

In order to calculate when a screw fractures during tightening Miller et al. [4] use the von Mises' formula for effective stress. Specifically, the screw fractures when the following force is applied:

$$P_{screw} = \sqrt{\sigma_{ys}^2 + 3\tau_{ys}^2}\left(\pi r_t^2\right) \tag{2.13}$$

where σ_{ys} is the tensile yield strength and τ_{ys} is the torsional yield strength. This formula allows them to convert the two different yield strengths into one effective yield strength, and then through algebraic manipulation find a force to cause failure. The force is then converted into a fail torque using the conversion equation (2.10)

$$T_{screw} = \sqrt{\sigma_{ys}^2 + 3\tau_{ys}^2}\left(\pi r_t^2\right)\left(\frac{\mu\cos\theta + \sin\theta\cos\beta}{\cos\theta\cos\beta - \mu\sin\theta}\left(\frac{D_s + D_h}{4}\right) + \mu\left(\frac{D_{sh} + D_n}{4}\right)\right). \tag{2.14}$$

The problem with this method lies in (2.13). This equation finds the force to cause failure by combining the force to cause torsional failure and the force to cause tensile failure. Although it is true that if this combined force were ever achieved the screw would fail, it still could fail at lower levels of force. If a purely torsional force is applied to the screw, and this torsional force is equal to the force required to achieve the torsional yield strength, then although the force would cause the screw to fail, the force would be less than the fail force found in (2.13) because the actual fail force would have no tensile component. Similarly a purely tensile force could cause the screw to fail without ever being at the level of the force found in (2.13).

For this reason we consider an alternative method of calculating the torque required to fracture a screw. Once again we consider von Mises' effective stress, however this time instead of applying it to the yield strengths, we use the formula to combine the applied torsional and tensile forces. By doing this we come up with a term for total effective stress, which we can then compare to the yield stress of the screw material.

From (2.7), we know the relationship between $F_{tensile}$ and $F_{torsional}$ where $F_{tensile} \equiv P$ and $F_{torsional} \equiv F$; we define their ratio to be γ

$$\frac{F_{tensile}}{F_{torsional}} = \frac{\cos\theta\cos\beta - \mu_1\sin\theta}{\mu_1\cos\theta + \sin\theta\cos\beta} = \gamma. \tag{2.15}$$

For a given screw geometry the ratio between tensile and torsional forces due to applied torque is fixed. The von Mises' formula effective stress on the screw cross sectional area A is then

$$\sigma' = \sqrt{\sigma^2 + 3\tau^2} = \sqrt{\frac{F_{tensile}^2}{A^2} + 3\frac{F_{torsional}^2}{A^2}} \tag{2.16}$$

where σ' is the effective stress, σ is the tensile stress, τ is the torsional stress, The cross sectional area of the screw shaft A is approximated by

$$A = \pi\left(\frac{D_p + D_r}{4}\right)^2.$$

Using γ, we solve for $F_{torsional}$ as a function of effective stress

$$\begin{aligned} \sigma' &= \frac{F_{torsional}}{A}\sqrt{\gamma^2 + 3} \\ F_{torsional} &= \frac{\sigma' A}{\sqrt{\gamma^2 + 3}}. \end{aligned} \tag{2.17}$$

By substituting σ' with our yield strength σ_{ys}, we find the torsional force required to break the screw,

$$F'_{torsional} = \frac{\sigma_{ys} A}{\sqrt{\gamma^2 + 3}}. \tag{2.18}$$

Since the torque used to tighten the screw can be represented by a torsional force, we can simply divide the applied torque by the radius at which it is being applied to find the torsional force to cause breaking:

$$T_{break} = \frac{\sigma_{ys} A D_p}{2\sqrt{\gamma^2 + 3}} \tag{2.19}$$

where D_p is the pitch diameter of the screw. The only problem is that we have to take into account the friction between the screw head and the near plate. Friction force is defined as the coefficient of friction multiplied by the force normal to the surface. In our case, the normal force is $F_{tensile}$ and therefore the friction force is:

$$F_{friction} = \mu_2 \gamma F_{torsional}. \tag{2.20}$$

While we are applying the torsional force (2.18) then, the frictional force is

$$F'_{friction} = \mu_2 \gamma \frac{\sigma_{ys} A}{\sqrt{\gamma^2 + 3}},$$

by (2.15) and the torque to overcome screw head friction is:

$$T'_{friction} = \mu_2 \gamma \frac{D_{sh} \sigma_{ys} A}{2\sqrt{\gamma^2 + 3}}, \tag{2.21}$$

where D_{sh} is the screw head diameter. We add the torque required to overcome screw head friction with the torque to break the screw to find the failure torque associated with screw breaking:

$$T_{Screw} = \frac{\sigma_{ys} A D_p}{2\sqrt{\gamma^2 + 3}} + \mu_2 \gamma \frac{\sigma_{ys} A D_{sh}}{2\sqrt{\gamma^2 + 3}}. \tag{2.22}$$

2.5.1 Machinery's Handbook Screw Fracture Method

Our method for modeling failure due to screw fracture is based on many of the same principles as the method presented in [3] though they are not the same. For completeness we include their method for calculating failure due to screw fracture.

According to [3], the fail torque T_{screw} due to screw fracture is defined as $T_{screw} = K F_{tensile} D_s$ where K is the torque coefficient defined as

$$K = \frac{1}{2D_s}\left(\frac{p}{\pi} + \mu_1 D_p \sec(\tan^{-1}(\tan\beta\cos\theta)) + \mu_2\left(\frac{D_s + D_h}{2}\right)\right). \tag{2.23}$$

Essentially, K serves the same purpose as γ in our method. The value for $F_{tensile}$ is found by using von Mises' effective stress as in our method only instead of solving for $F_{torsional}$ the equation is solved for $F_{tensile}$:

$$F_{tensile} = \frac{\sigma_{ys} A}{\sqrt{1 + 3\left[\frac{2}{D_p}\left(\frac{p}{\pi} + \mu_1 D_p \sec(\tan^{-1}(\tan\beta\cos\theta))\right)\right]^2}}. \tag{2.24}$$

Thus, the fail torque from screw fracture is:

$$T_{screw} = \frac{\frac{1}{2}\left(\frac{p}{\pi} + \mu_1 D_p \sec(\tan^{-1}(\tan\beta\cos\theta)) + \mu_2\left(\frac{D_s+D_h}{2}\right)\right)\sigma_{ys}A}{\sqrt{1+3\left[\frac{2}{D_p}\left(\frac{p}{\pi} + \mu_1 D_p \sec(\tan^{-1}(\tan\beta\cos\theta))\right)\right]^2}} \tag{2.25}$$

2.6 Joint Failure Method

Now that we have the three different torques required to achieve the three different methods of failure, we need to find the relationship between the torque we apply from our screwdriver and each of the three fail torques. Physically, the applied torque is being split among the three different failure types so that no one failure type is getting all of the applied torque. Unfortunately, we do not know how the force is being distributed between the three types of failure. To find out which of three methods of failure will cause the joint to fail, that is the joint failure method, we would simply take the minimum of the three different fail torques, (2.11), (2.12), and (2.22) multiplied by the appropriate factors. Future research should be done into finding exactly how the applied torque is distributed among the different failure methods. For now we assume that each type of failure is having all of the applied torque placed on it. This will always underestimate our fail torques, however we feel that this is better than overestimating them and having screws fail unexpectedly.

To resolve this issue in the model for BOSE, we allowed for a torque ratio variable to be used to distribute the torques. The torque ratio for each method of failure determines what fraction of the applied torque is going into that method of failure. Theoretically the sum of all of the fail torques should equal one, however for the sake of simplicity we did not make that required in the GUI. By default, each method of failure receives the full applied torque as suggested by the REU, however this can be changed by the user of the program; see Figure 2.6.

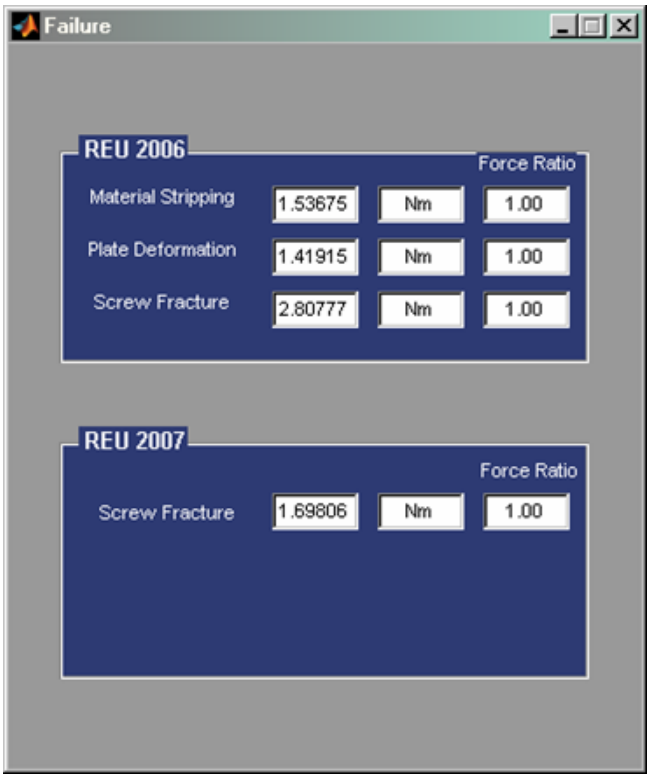

Figure 2.6: Failure GUI programmed with the failure model from CIMS REU 2006 and REU 2007

Chapter 3

Clamp Load

3.1 Introduction

The purpose of a fastener is to keep two plates attached to each other such that they will stay together while forces are applied to them. A screw fulfills that purpose by creating a *clamp load* in the joint. Clamp load is the force created by tightening a screw that compresses the plates in the joint; see Figure 3.1. Although the clamp load is created when the screw is being tightened, the force acts on the joint throughout its lifespan. The clamp load acts as a compressive force on the plates and as a tensile force on the screw, causing the plates to compress and the screw to stretch axially. Typically a desired clamp load is 75% of the ultimate tensile strength for dynamically loaded bolts and 90% of the ultimate tensile stength for statically loaded bolts [9].

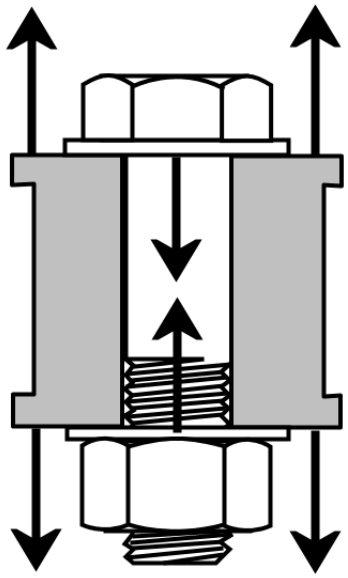

Figure 3.1: Clamp load forces acting on a bolt, nut, and plate system.

Clamp load is created by the tightening of the screw; as the screw is tightened it is stretched axially, and undergoes an elastic deformation. When the tightening is complete the screw attempts to return to the original shape, which causes a force to be applied to the plates. Likewise, during tightening of the screw the plates are being compressed in the elastic region, and when tightening is complete the plates attempt to return to their original shape. These two forces create an equilibrium in the system. Clamp load is a linear function of torque until we reach the point of tightening where the joint materials undergo a stress equal to their yield strength; see Figure 3.2.

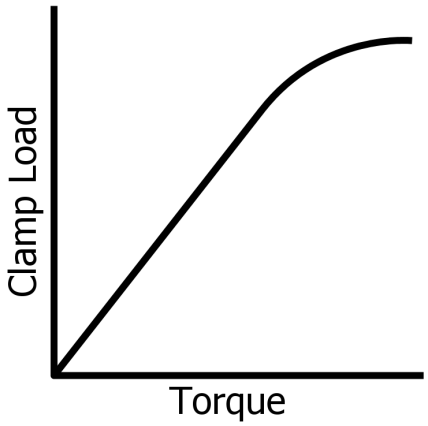

Figure 3.2: Graph of torque versus clamp load generated.

When an outside force acts to separate the plates it must first counteract the clamp load in the system. For this reason having a high clamp load is beneficial; it will allow the joint to withstand higher forces. Though it is desirable to have a high clamp load, if the screw is over-tightened, plastic deformation may occur. We prefer to never reach this point of permanent deformation since it would result in the loss of clamp load. It is desirable for BOSE to have an algorithm for finding the required torque to attain a given clamp load in a joint as well as a method for finding the clamp load in a joint for a given torque.

3.2 Techniques for Finding Clamp Load

Since clamp load is a force acting internally in a joint, it is not something that can be directly measured. The most common methods for finding a clamp load involve measuring the physical properties of the joint and inferring the clamp load from those results. There are several different methods for making this calculation that are used in modern machining; the most common methods according to [6] are given.

3.2.1 Elongation Measurement

Since the clamp load causes the screw to stretch, one method of measuring clamp load is to measure the amount of elongation of the screw during or after tightening. The amount of elongation can then be used to find the strain of the screw. Using Young's Modulus, the amount of tensile force on the screw can be obtained. Young's Modulus E is defined as:

$$E = \frac{\sigma}{\varepsilon}, \tag{3.1}$$

where σ is applied stress and ε is strain or the elongation per unit length caused by the stress. If the screw has both ends accessible then it is possible to simply measure the amount of elongation with a micrometer. In other situations ultrasonic transducers can measure the elongation from solely the head of the screw.

3.2.2 Torque Measurement

Another common method of measuring clamp load is to measure the amount of torque required to tighten the screw. Torque wrenches allow for tightening to stop once a designated torque is achieved, and from the torque value the amount of force in the system can be calculated using an equation to define the torque to force relationship. This method is prone to error due to the torque wrenches having inaccuracies of up to 30%.

3.2.3 Turn-of-the-Nut Method

The Turn-of-the-Nut Method is a method of clamp load calculation that relies on indirectly measuring screw elongation by using the amount of rotation beyond seating undergone by the head of the screw. The screw is inserted into the joint until the head is flush with the near plate. The screw is then tightened by amount $\Delta\phi$. The rotation of the screw is used in conjunction with the screw thread helix angle θ and pitch length p to calculate the amount of elongation that the screw has undergone. That elongation can then be used to calculate the clamp load as done in 3.2.1. This method is advantageous in that it requires no special measuring tools, simply the precise amount of rotation that has been applied to the screw. This method first became popular shortly after World War II [9].

3.3 Computing Clamp Load

For our algorithm we require a method of calculating the clamp load in the joint when the screw is tightened to a given torque. We formally define this question as: given a torque $\hat{T}$ such that $T_{drive} \leq \hat{T} \leq T_{fail}$ what is the clamp load F_{clamp} in the joint? The calculation must be based on input by the user and cannot be based on experimental data. Unfortunately the most common methods of estimating clamp load are not nearly as accurate as experimentally measuring the clamp load. This is largely due to factors such as the operator error or minor defects in the screw that cannot be calculated. Also, most research on clamp load has only been done for bolts; there is very little literature on the clamp load of self-tapping screws.

Although much of the literature on clamp load in a bolt can be applied to a self-tapping screw, there are differences between the two fasteners that must be considered. A bolt/nut system has a threaded bolt inserted into a nut that has been threaded to fit the bolt. The nut is lubricated to minimize friction so that the bolt is easier to tighten. A bolt has a long shaft that does not come into contact with the plates that are being fastened; there is no friction between the bolt and the plates. A self-tapping screw does not have a nut to fasten it, rather the threads of the screw engage the tap plate. In this regard the tap plate is similar to the nut of a bolt/nut joint, however the tap plate is often made of weaker materials than a nut, so deformation of the tap plate has to be considered in the clamp load calculation. The near plate of the self-tapping screw is equivalent to all of the plates in the bolt/nut joint, since the near plate does not come into contact with the shaft or the threads of the screw. Since the near plate has the possibility of being very thin, it is possible that a self-tapping screw has only a very short length of the shaft that is not engaged to the thread. In this situation there is only a short amount of the screw that can freely stretch, which is typically not a problem in a bolt/nut joint.

3.3.1 Model 1

In our first model we base our calculation on the turn-of-the-nut method. Using the model in [5] and [8], we calculate the rotation ϕ required to achieve a specific tightening torque, $\hat{T}$. In [5] the tightening torque is dependent on the friction between the threads of the screw and the tap plate, the friction between the head of the screw and the near plate, and the force required to stretch the screw because of tightening. We use their calculations to find the amount of rotations until the desired torque is achieved, $\hat{\phi}$. The screw is seated at ϕ_t rotations where

$$\phi_t = \frac{2\pi l}{p}, \tag{3.2}$$

p is the pitch length of the screw, and l is the length of the screw. The amount of rotation done during tightening is then $\delta\phi = \hat{\phi} - \phi_t$. We then convert rotation of the screw to elongation of the screw. This conversion is simplified by assuming that all rotation results in elastic stretching of the screw and no deformation of the near plate or the tap plate. Considering the thread helix angle θ of the screw, elongation e is given by

$$e = \frac{p\delta\phi}{2\pi}$$

from which we can calculate the strain of the screw:

$$\varepsilon = \frac{e}{l}.$$

Using the Young's Modulus of the screw (3.1), we have

$$\sigma = E\varepsilon.$$

Since force is stress times area, we can use the cross sectional area of the screw to find the tensile force being applied. This gives us a final equation for clamp load

$$F_{clamp} = \frac{p\delta\phi EA}{2\pi l} \tag{3.3}$$

where A is the cross sectional area of the screw shaft. This equation allows us to estimate clamp load by using the material properties of the screw as well as how much we have tightened it. However, it is a simplification of the problem because it fails to take into account any deformation of the system besides the screw elongating axially. It is possible that tightening the screw is causing torsion of the screw or deformation of the threads in the near plate, however Model 1 does not take these forces into account.

3.3.2 Model 2

Another approach to calculating the clamp load of our joint is to use the tightening torque directly. Clamp load can be found as a function of torque as follows from [1]:

$$\hat{T} = F_{clamp}\left(\frac{p}{2\pi} + \frac{\mu_1}{\cos\beta}\left(\frac{D_s + D_h}{4}\right) + \mu_2\left(\frac{D_n + D_{sh}}{4}\right)\right). \tag{3.4}$$

Here the $\frac{p}{2\pi}$ term is produced by the tensile force being applied to the screw by stretching. The second term $\frac{\mu_1}{\cos\beta}\left(\frac{D_s+D_h}{4}\right)$ models the friction between the screw thread and tap plate. The final term in the equation

$\mu_2\left(\frac{D_h+D_{sh}}{4}\right)$ represents the friction between the screw head and near plate. The equation (3.4) is similar to (2.10) to find the relationship between torque and force causing failure. This similarity is due to the fact that both equations are attempting to find a tensile force created by an applied torque on the screw. The main difference in the equations is the friction terms. The friction term in (3.4) seems to take $\theta = 0$.

By solving this equation for F_{clamp}, we find the clamp load of the joint as a function of torque. This method has the same problem as model 1 where it is assumed that there is no torsion nor screw deformation involved in tightening. The advantage of this method is that it does not require measuring of the angle used to tighten, so there is one less source of error.

3.3.3 Model 3

A third approach for calculating clamp load is given by [3]. This method calculates the clamp load specifically at the point of screw failure. The yield clamp load F'_{clamp} is as follows:

$$F'_{clamp} = \frac{\sigma_y A}{\sqrt{1+3\left[\frac{4}{D_p}\left(\frac{p}{\pi}+\mu_1 D_p \sec(\tan^{-1}(\tan\beta\cos\theta))\right)\right]}} \tag{3.5}$$

This model has similarities to the work done in Section 2.5 with von Mises' effective stress. Like (2.5) von Mises' effective stress is used to find the amount of force within the system at the point of failure of the screw. The main difference in (3.5) is that rather than finding the torsional force, the tensile force is found since that is the clamp load of the joint. Another difference is that instead of the ratio γ (2.15) that is used to related the tensile and torsional forces, [3] uses $\frac{p}{\pi}+\mu_1 D_p \sec(\tan^{-1}(\tan\beta\cos\theta))$.

3.3.4 Conclusion

Both model 1 and model 2 provide viable methods of estimating the clamp load in a joint held by a self-tapping screw. Model 3 is also useful for finding the clamp load at screw failure. A possible area for future work would be to investigate how much clamp load is lost in a self tapping screw due to torsion. Also the question remains of how much stretching changes the geometry of the screw, especially θ, which would affect further tightening.

Chapter 4

Heat Transfer

4.1 Introduction

The initial torque models in [5] and [8] assume that no heat is generated in the screw insertion process. However, as suggested in [5], the discrepancy between the theoretical and experimental torque curves may be partly attributed to heat effects. We find this conjecture feasible since a significant amount of torque required for screw insertion goes towards overcoming friction, and it is widely accepted that nearly all of the energy dissipated in friction is transformed into heat [7]. Our goal then is to investigate how heat generated by friction affects material properties, and to incorporate these changes into the calculation for insertion torque.

We will consider all energy expended on overcoming kinetic friction to be generated heat. We do not consider any heat generated in the cutting (displacement) process because we were not able to research how much displacement energy is transformed into heat. We also do not consider any heat generated during engagement or tightening because the rotation intervals are very small. Therefore, we consider heat generated by friction for $\alpha < \overline{\phi} < \phi_t$ only, the interval during which the untapered portion of the screw is engaged in the tap plate material. Recall, $\overline{\phi}$ is the amount of rotation completed which corresponds to the depth of the screw in the tap plate.

The ultimate strength of the material depends on temperature, so variations in temperature cause changes in the friction forces and thus, the torque required to overcome friction. Since the total torque required for insertion is the sum of the torques required for engagement, displacement, friction, and tightening, the entire torque curve will be modified when we account for heat.

In [4], a method of modeling heat generated by friction during screw insertion is developed. For the model, they assume instantaneous heat distribution, and uniform temperature of the screw. Thus, time and speed of insertion are not factors in their model; only the physical properties of the screw and plate are considered relevant. Two different models are presented in [4]. In the first model, they assume that all the heat generated by insertion enters the screw. The quantity of heat entering the screw at every insertion position $\bar{\phi}$ is computed. They then convert the heat generated into change in temperature of the screw to find the temperature of the screw for each $\bar{\phi}$. Finally from these temperatures they find the ultimate tensile strength of the material around the screw at the temperature of the screw, which allowed them to include heat in the insertion model of [5].

The second model does not assume that heat enters only the screw. Instead, some of the heat is assumed to enter the material surrounding the screw as well. They assume that the volume of plate material around the screw that experiences a temperature change around the screw is shaped like a cone and that, as the

screw is inserted further into the material, the cone volume expands. They find that due to the low thermal conductivity of a plastic tap plate relative to that of a metal screw the amount of heat that enters the tap plate is negligible. For this reason, it is reasonable to assume that no heat enters the plastic tap plate.

For our model, we relax the assumption of instantaneous heat diffusion and uniform temperature. By relaxing this assumption, the speed at which the screw is inserted becomes a factor in the model. To model the temperature dynamics within the screw, we use the heat equation, a partial differential equation, along with appropriate boundary and initial conditions.

4.2 Posing the Problem

4.2.1 Heat Equation

The fundamental heat equation is as follows:

$$\frac{\partial \mathscr{T}}{\partial t}(\mathbf{x},t) = \frac{1}{\rho c}\nabla \cdot (K\nabla \mathscr{T}). \tag{4.1}$$

This equation defines the temperature $\mathscr{T}$ at position $\mathbf{x}$ at time t in the system. Here K is the thermal conductivity of the material, ρ is the material density, and c is the specific heat capacity of the material. We use this partial differential equation, along with appropriate initial and boundary value problems to model the temperature variation in the screw.

To simplify the geometry of the problem, we approximate the screw by a cylinder of diameter D_r and height $L - L_t$ where D_r is the root diameter of the screw, L is the length of the screw, and L_t is the length of the tapered portion of the screw. This approximation removes the thread of the screw as well as the untapered region of the screw so that the region of interest has a geometrically simpler boundary. See Figure 4.1. In cylindrical coordinates [1], this cylinder is defined as

$$\begin{aligned} 0 &\le \gamma \le 2\pi \\ 0 &\le r \le D_r/2 \\ 0 &\le z \le L - L_t. \end{aligned}$$

When the thermal conductivity is independent of temperature, the heat equation in cylindrical coordinates is given by

$$\frac{\partial \mathscr{T}}{\partial t} = \frac{K}{\rho c}\left(\frac{\partial^2 \mathscr{T}}{\partial r^2} + \frac{1}{r}\frac{\partial \mathscr{T}}{\partial r} + \frac{1}{r^2}\frac{\partial^2 \mathscr{T}}{\partial \gamma^2} + \frac{\partial^2 \mathscr{T}}{\partial z^2}\right). \tag{4.2}$$

4.2.2 Boundary Regions

Since there are no threads in our model (cylindrical) screw, we assume that the friction region is the projection of the portion of the threads engaged with the tap plate projected onto the cylinder. The surface of our cylinder is split into four regions; see Figure 4.2. The bottom of the screw shaft is denoted B_1; likewise the top of the cylinder which represents the top of the screw shaft is denoted B_4. The central face is split into two regions, B_2 and B_3. The region representing the thread generating heat from friction is B_2 while the region that is not generating heat is B_3. The conductivity of plastic is typically significantly less than the conductivity of metal, so we assume that the amount of heat entering the tap plate is negligible. For this

[1] we use γ for our azimuthal angle instead of the traditional θ since we have defined θ as the thread helix angle

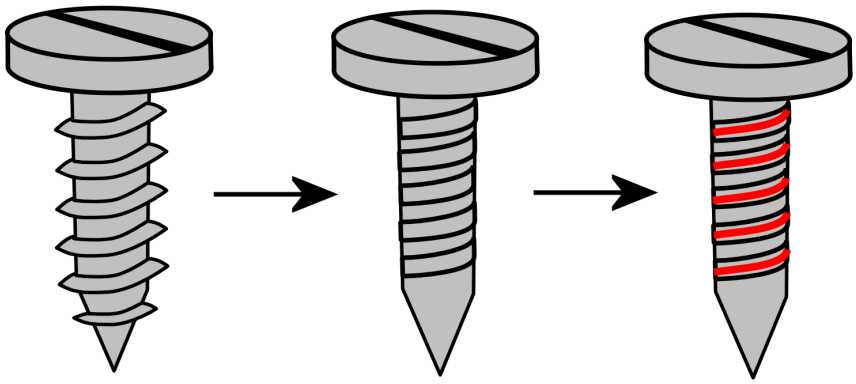

Figure 4.1: Simplified screw geometry for heat calculation. The heat generating region is shown in red.

reason, we consider B_1 and B_3 to be insulated. The heat flux in region B_4 is dependent on how much heat is being absorbed by the head of the screw and how much of that heat is being lost into the air. In this work, we assume B_4 is also insulated, however this is a topic requiring further research. It is straightforward to define the regions B_1 and B_4:

$$B_1 = \begin{cases} 0 \leq \gamma \leq 2\pi \\ 0 \leq r \leq \frac{D_r}{2} \\ z = 0 \end{cases} \tag{4.3}$$

$$B_4 = \begin{cases} 0 \leq \gamma \leq 2\pi \\ 0 \leq r \leq \frac{D_r}{2} \\ z = L - L_t \end{cases}. \tag{4.4}$$

However, defining B_2 and B_3 is more complicated. Region B_2 is a helical strip around the side of the cylinder. In order to define it, we find the width of the strip. Recall that the strip is the projection of the engaged thread onto the cylinder. By analyzing the cross section of the thread, we find that the height of the strip is $\frac{1}{2}(\tan\beta_1 + \tan\beta_2)(D_s - D_h)$; see Figure 4.3. Since we know that the ratio of width to height must be the same as $\pi D_r : p$ our value for the width of the strip is

$$\frac{\pi(\tan\beta_1 + \tan\beta_2)(D_s - D_h)D_r}{2p},$$

so the angular width is

$$\frac{\pi(\tan\beta_1 + \tan\beta_2)(D_s - D_h)}{p}.$$

From here we can define B_2 as

$$B_2 = \begin{cases} \left(\frac{2\pi z}{p} \leq \gamma \leq \frac{2\pi z + \pi(\tan\beta_1 + \tan\beta_2)(D_s - D_h)}{p}\right) \mod 2\pi \\ r = \frac{D_r}{2} \\ 0 \leq z \leq L - L_t \end{cases}. \tag{4.5}$$

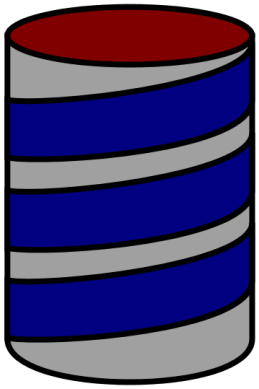

Figure 4.2: The boundaries of the cylinder: B_2 is the blue region, B_3 is the gray region, B_4 is the red region, and B_1 is not shown.

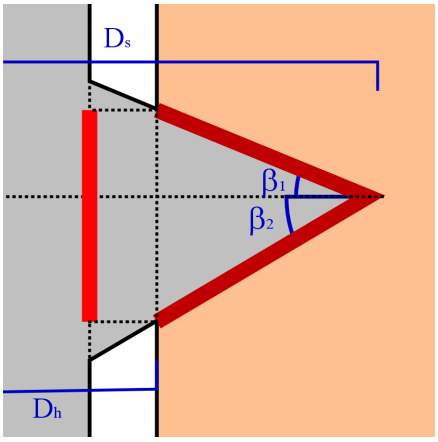

Figure 4.3: Cross section of screw during heat generation. The maroon segment represents the true heat generating surface and the red represents our projection onto the cylinder.

We now define region B_3. Since $B_2 \cup B_3$ is just the surface of the side of the cylinder, we simply define B_3 as the surface of the side of the cylinder with set B_2 removed:

$$B_3 = (B_2 \cup B_3) \setminus B_2. \tag{4.6}$$

4.2.3 Boundary Conditions

We consider our boundary to be of two types. There are two conditions on the boundaries; some of the screw boundary is insulated, while the area representing the screw thread engaged to the tap plate is generating heat. For the insulated region, there is no heat flow across the boundary so the boundary condition is $\frac{\partial \mathscr{T}}{\partial n} = 0$. For the heat generating portion, we use Fourier's Law which relates heat flux to the directional derivative of temperature.

Since heat is a form of energy, we use the equation for work to find how much energy is generated

$$\begin{aligned} \text{Work} &= \text{Force} \times \text{Displacement} \\ Q &= F_{friction} \times d. \end{aligned} \tag{4.7}$$

Our force term for friction $F_{friction}$ is dependent on the normal force F_N that the screw exerts on the tap plate. The displacement refers to the change in position of the force. For our screw the force is moving in a helical manner as the screw is inserted into the tap plate. Since we know that this force is strong enough to cut the material we find the force as a function of the ultimate tensile strength σ_{uts} of the tap plate material,

$$\begin{aligned} \sigma_{uts} &= \frac{F_N}{A} \\ F_N &= \sigma_{uts} A \\ F_{friction} &= \mu \sigma_{uts} A, \end{aligned} \tag{4.8}$$

where μ_1 is the coefficient of friction between the screw and tap plate and A is the area of the region generating heat. We also must find out how much displacement will occur. Since the area generating friction is on the surface of the screw, we find the amount of displacement that a point on the screw will undergo in time t; see Figure 4.4. In time t, the screw will rotate a distance of $2\pi t \omega \frac{D_r}{2}$, where ω is the revolutions per second of the screw. A point on the screw is not just spinning but moving on a helix so we take that into account by dividing by $\cos\theta'$ to get

$$d = \frac{2\pi t \omega \frac{Dr}{2}}{\cos\theta'}. \tag{4.9}$$

Note that we use θ' rather than θ because since our cylinder has a smaller diameter than D_s the thread helix angle on our cylinder will be different than the thread helix angle measured from the tip of the thread. With (4.7), (4.8) and (4.9), our equation for work is

$$Q = \frac{\pi \mu_1 \sigma_{uts} A t \omega D_r}{\cos\theta'}. \tag{4.10}$$

From (4.10), the heat flux, that is, the rate at which heat flows across a unit area of surface, is

$$q = \frac{\pi \mu_1 \sigma_{uts} \omega D_r}{\cos\theta'}. \tag{4.11}$$

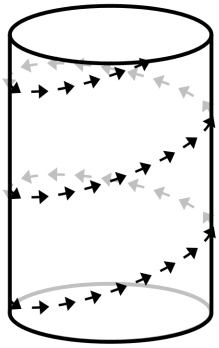

Figure 4.4: The path of a force generating friction on the surface of our cylinder.

Fourier's Law of Heat Conduction gives

$$q = -K\frac{\partial \mathscr{T}}{\partial n}, \tag{4.12}$$

so using (4.11), we find that where there is frictional heating, the boundary condition is

$$\frac{\partial \mathscr{T}}{\partial n} = -\frac{\mu_1 \sigma_{uts} \pi \omega D_r}{K \cos\theta'}. \tag{4.13}$$

Surfaces B_1, B_3, and B_4 are insulated surfaces. The surface B_2 is heat-generating but only at positions that are in contact with the tap plate. For this reason, a point on the surface B_2 at height z on the model cylinder at time t after the untapered region contacts the tap plate will only generate heat when $t\omega p - t_2 \leq z \leq t\omega p$ where t_2 is the length of the tap plate, since if $z \leq t\omega p - t_2$ then the point will have broken through the tap plate, and if $t\omega p \leq z$ the point will not yet have entered the tap plate.

In summary, we model heat generation and temperature distribution during the self-tapping screw insertion process by the following initial value boundary problem:

$$\frac{\partial \mathscr{T}}{\partial t} = \frac{K}{\rho c}\left(\frac{\partial^2 \mathscr{T}}{\partial r^2} + \frac{1}{r}\frac{\partial \mathscr{T}}{\partial r} + \frac{1}{r^2}\frac{\partial^2 \mathscr{T}}{\partial \gamma^2} + \frac{\partial^2 \mathscr{T}}{\partial z^2}\right)$$

$$\frac{\partial \mathscr{T}}{\partial n} = \begin{cases} 0 & (\gamma, r, z) \in B_1, B_3, B_4 \\ -\frac{\mu_1 \sigma_{uts} \pi \omega D_r}{K \cos\theta'} & (\gamma, r, z) \in B_2 \qquad t\omega p - t_2 \leq z \leq t\omega p \\ 0 & (\gamma, r, z) \in B_2 \qquad z \leq t\omega p - t_2 \\ 0 & (\gamma, r, z) \in B_2 \qquad t_2 \omega p \leq z \end{cases}. \tag{4.14}$$

$$\mathscr{T}(\gamma, r, z, 0) = \mathscr{T}_{init},$$

$$0 \leq \gamma \leq 2\pi, \qquad 0 \leq r \leq D_r/2, \qquad 0 \leq z \leq L - L_t, \qquad t \geq 0.$$

We take $\mathscr{T}_{init}$ to be room temperature.

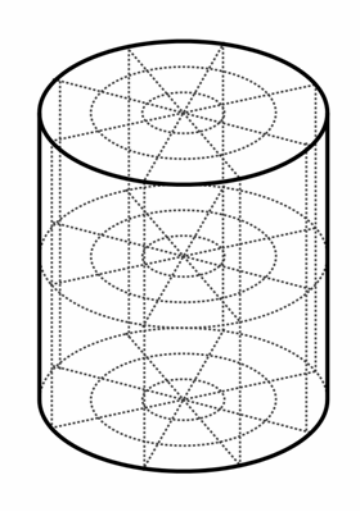

Figure 4.5: A cell used in the numerical method for solving the heat equation in a cylinder.

4.3 Numerical Methods

We solve the initial value boundary problem above numerically. The model cylinder is discretized into discrete cell volumes; see Figures 4.5 and 4.6. Choosing positive integers N_γ, N_r, N_z, the cell volumes each have dimensions $\Delta\gamma = 2\pi/N_\gamma, \Delta r = D_r/2N_r, \Delta z = (L-L_t)/N_t$. In addition, we discretize the time into steps of size Δt so that $t_n = n\Delta t$.

We use a finite volume methodology. The temperature at the center of cell (i,j,k) for $i = 1,\cdots,N_\gamma$, $j = 1,\cdots,N_r$ and $k = 1,\cdots,N_z$ is denoted by

$$\mathscr{T}^n_{i,j,k} \approx \mathscr{T}((i-1/2)\Delta\gamma, (j-1/2)\Delta r, (k-1/2)\Delta z, n\Delta t),$$

and is taken to be the average temperature in that cell. To derive the numerical scheme that computes $\mathscr{T}^{n+1}_{i,j,k}$, we use the law of conservation of energy. The amount of heat energy in the (i,j,k)th cell at time t_{n+1} is equal to the heat energy in the cell at t_n plus the heat enters the cell via its faces between time t_n and time t_{n+1}. Equivalently, we integrate the heat equation over the cell volume

$$\iiint_R \rho c \frac{\partial \mathscr{T}}{\partial t} dV = \iiint_R \nabla \cdot (K \nabla \mathscr{T})\, dV \tag{4.15}$$

which, for constant ρ, c, and K gives

$$\frac{\partial}{\partial t}\iiint_R \rho c \mathscr{T}\, dV = \iint_{\partial R} K \nabla \mathscr{T} \cdot \vec{n}\, dA \tag{4.16}$$

$$= \iint_{R_1} \frac{\partial \mathscr{T}}{\partial n} dA + \iint_{R_2} \frac{\partial \mathscr{T}}{\partial n} dA + \iint_{R_3} \frac{\partial \mathscr{T}}{\partial n} dA + \\ + \iint_{R_4} \frac{\partial \mathscr{T}}{\partial n} dA + \iint_{R_5} \frac{\partial \mathscr{T}}{\partial n} dA + \iint_{R_6} \frac{\partial \mathscr{T}}{\partial n} dA, \tag{4.17}$$

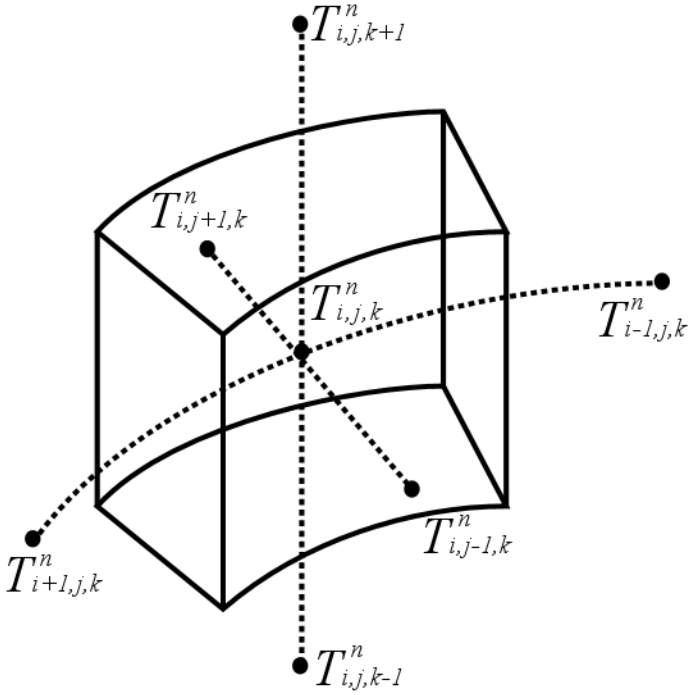

Figure 4.6: A cell used in the numerical method for solving the heat equation in a cylinder.

for a typical cell volume with six boundary faces which we denote by $R_1, \cdots, R_6$. The mean value theorem for integrals gives

$$\frac{\rho c}{K}|R|\frac{\partial \hat{\mathscr{T}}}{\partial t} = \frac{\partial \hat{\mathscr{T}}_1}{\partial n}|R_1| + \frac{\partial \hat{\mathscr{T}}_2}{\partial n}|R_2| + \frac{\partial \hat{\mathscr{T}}_3}{\partial n}|R_3| + \frac{\partial \hat{\mathscr{T}}_4}{\partial n}|R_4| + \frac{\partial \hat{\mathscr{T}}_5}{\partial n}|R_5| + \frac{\partial \hat{\mathscr{T}}_6}{\partial n}|R_6| \tag{4.18}$$

where $\hat{\mathscr{T}}$ is the average temperature in the volume and $\frac{\partial \hat{\mathscr{T}}_i}{\partial n}$ is the average outward normal derivative on R_i. The areas and volumes considered are inserted into the formula, and the partial derivatives are replaced with their numerical approximations

$$\begin{aligned}\frac{\rho c}{K}\frac{\mathscr{T}^{n+1}_{i,j,k} - \mathscr{T}^n_{i,j,k}}{\Delta t} r_j \Delta r \Delta\gamma \Delta z \quad \approx \quad & \frac{\mathscr{T}^n_{i+1,j,k} - \mathscr{T}^n_{i,j,k}}{r_j \Delta\gamma}\Delta r \Delta z + \frac{\mathscr{T}^n_{i,j,k} - \mathscr{T}^n_{i-1,j,k}}{r_j \Delta\gamma}\Delta r \Delta z + \\ & + \frac{\mathscr{T}^n_{i,j+1,k} - \mathscr{T}^n_{i,j-1,k}}{\Delta r}(r_j + \frac{\Delta r}{2})\Delta\gamma \Delta z + \frac{\mathscr{T}^n_{i,j,k} - \mathscr{T}^n_{i,j-1,k}}{\Delta r}(r_j - \frac{\Delta r}{2})\Delta\gamma \Delta z + \\ & + \frac{\mathscr{T}^n_{i,j,k+1} - \mathscr{T}^n_{i,j,k}}{\Delta z} r_j \Delta r \Delta\gamma + \frac{\mathscr{T}^n_{i,j,k} - \mathscr{T}^n_{i,j,k-1}}{\Delta z} r_j \Delta r \Delta\gamma. \end{aligned} \tag{4.19}$$

See Figure 4.6 to see the locations of the cells surrounding $\mathscr{T}^n_{i,j,k}$. When simplified and solved for $\mathscr{T}^{n+1}_{i,j,k}$ (4.19) becomes:

$$\begin{aligned}\mathscr{T}^{n+1}_{i,j,k} \approx \kappa \Delta t \Big(& \frac{\mathscr{T}^n_{i,j+1,k} - 2\mathscr{T}^n_{i,j,k} + \mathscr{T}^n_{i,j-1,k}}{(\Delta r)^2} + \frac{1}{r_j}\frac{\mathscr{T}^n_{i,j+1,k} - \mathscr{T}^n_{i,j-1,k}}{2\Delta r} + \\ & + \frac{1}{r_j^2}\frac{\mathscr{T}^n_{i+1,j,k} - 2\mathscr{T}^n_{i,j,k} + \mathscr{T}^n_{i-1,j,k}}{(\Delta\gamma)^2} + \frac{\mathscr{T}^n_{i,j,k+1} - 2\mathscr{T}^n_{i,j,k} + \mathscr{T}^n_{i,j,k-1}}{(\Delta z)^2}\Big) + \mathscr{T}^n_{i,j,k} \end{aligned} \tag{4.20}$$

where $\kappa = K/\rho c$ is known as the thermal diffusivity.

We now have a method for finding temperature at $\mathscr{T}_{i,j,k}^{n+1}$ in terms of temperatures at time n. This is an explicit scheme since we can define $\mathscr{T}_{i,j,k}^{n+1}$ solely in terms of temperatures at time t_n. Starting with the initial values at time $n = 0$ we can systematically solve for temperatures at time $n = 1$, $n = 2$, and so on until we have temperature values for all of the cells at all of the times during screw insertion. To ensure stability, we use a value for Δt that is small enough to satisfy stability criterion for explicit schemes for diffusion equations. For our scheme (4.20), that condition is

$$\Delta t \kappa \left(\frac{1}{(\Delta r)^2} + \frac{1}{(\Delta \gamma r_j)^2} + \frac{1}{(\Delta z)^2} \right) \leq \frac{1}{2}. \tag{4.21}$$

4.4 Interfacing our Model with Previous Work

Ultimately, we are not concerned with the temperature of the screw, but rather the ultimate tensile strength of the material surrounding the screw thread. Since ultimate tensile strength is a function of temperature, if we can find the temperature of the material surrounding the screw we can find the ultimate tensile strength of that material. Since the tap plate is in contact with the heat-generating portions of the thread, we use the temperature of the surface of the screw along the thread for the value of the temperature of the tap plate.

The work done by Leo et al. in [5] finds the amount of torque required to overcome friction by computing an integral along ϕ where ϕ is the helix coordinate variable of the screw. Inside that integral is a term for ultimate tensile strength. For this reason, it would be helpful to find the ultimate tensile strength of the material as a function of ϕ and $\bar{\phi}$ where $\bar{\phi}$ is the angular position at the top of the tap plate. Then, we replace the standard ultimate tensile strength term in the integral with the function and compute the integral numerically.

First, we find a function $\mathscr{T}'(\phi,t)$ that gives the temperature of the screw thread at point ϕ at time t. We define $\mathscr{T}'(\phi,t)$ as

$$\mathscr{T}'(\phi,t) = \frac{D_r \pi (\tan\beta_1 + \tan\beta_2)(D_s - D_h)}{p} \int_{\frac{2\pi z}{p}}^{2\pi z/p + \pi(\tan\beta_1+\tan\beta_2)(D_s-D_h)/p} \mathscr{T}\left(\gamma, \frac{D_r}{2}, \frac{2\pi\phi + L_t}{p}, t\right) d\gamma \tag{4.22}$$

when $\phi > \frac{2\pi L_t}{p}$ and is equal to $\mathscr{T}_{init}$ otherwise. The next step is to remove the time component of the function and replace it with $\bar{\phi}$, where $\bar{\phi}$ is the point ϕ at the top of the tap plate. This is done because the model proposed in [5] has no time component; rather it measures the insertion process by what point ϕ is currently at the top of the tap plate. Therefore

$$\mathscr{T}_2'(\phi,\bar{\phi}) = \mathscr{T}'\left(\phi, \frac{\bar{\phi}}{2\pi\omega}\right). \tag{4.23}$$

Now that we have a temperature function of ϕ and $\bar{\phi}$ we need to convert it to a function of ultimate tensile strength. Research done in [4] finds that a linear relation exists between ultimate tensile strength and temperature. Using data found in [2], a least squares method is used to obtain the following equation

$$\sigma_{uts}(\mathscr{T}) = s_1 \mathscr{T} + s_0 \tag{4.24}$$

where s_0 and s_1 are least squares coefficients. We substitute $\mathscr{T}_2'(\phi,\bar{\phi})$ for $\mathscr{T}$ to get

$$\sigma_{uts}(\phi,\bar{\phi}) = s_1 \mathscr{T}_2'(\phi,\bar{\phi}) + s_0. \tag{4.25}$$

With (4.25), we have a term that can be used to replace σ_{uts} in the equations done in [5] to implement our heat model.

4.5 Other Concerns

4.5.1 Improving Friction Term

In 4.4, we found a method of relating temperature to ultimate tensile strength. Although this is important for interfacing our heat model with the work done in [5], it has another application as well. To find the amount of heat generated during screw insertion we have a term for ultimate tensile strength (4.13). With slight modification (4.14) can be used to find the ultimate tensile strength for the boundary condition, which would make our model more accurate. The new boundary condition ends up as:

$$\frac{\partial \mathscr{T}}{\partial n} = \begin{cases} 0 & (\gamma, r, z) \in B_1, B_3, B_4 \\ -\frac{\mu_1 \sigma_{uts}(z,t)\pi\omega D_r}{K\cos\theta'} & (\gamma, r, z) \in B_2 \qquad t\omega p - t_2 \leq z \leq t\omega p \\ 0 & (\gamma, r, z) \in B_2 \qquad z \leq t\omega p - t_2 \\ 0 & (\gamma, r, z) \in B_2 \qquad t_2\omega p \leq z \end{cases} . \tag{4.26}$$

4.5.2 Tightening

Our model generates heat in the screw by considering how much displacement a point on the screw thread undergoes. During the tightening phase of screw insertion, the displacement of a point on the screw thread can vary depending on if the tightening is causing the screw to stretch and if the head of the screw is limiting movement. Due to the complex nature of finding the exact amount of displacement during tightening, we chose to not consider heat diffusion during the tightening phase. Instead, we hold the temperature of the screw constant during tightening. Further research should be done into heat generated during tightening in order to find a more accurate method of representing temperature.

4.5.3 Heat Generating Area

A source of error in our model is the location of the heat generating surface. By projecting the surface onto a cylinder, the area of the surface has decreased. Not only that, but since the surface is now closer to the center of the cylinder, the surface travels less when the screw is rotated; see Figure 4.7. For these reasons the amount of heat generated in our model is inaccurate. A more accurate model for how much heat is generated was created by [4], however their model was not conducive to an initial value boundary problem, so we did not use it. When the amount of heat generated by their model is compared to ours using equivalent screws and tap plate materials, it is found that their screw had a temperature change of 37.25°C while our screw had an average temperature change of 16.8°C. Further research should be done into modifying our heat generating term so that it is closer to that in [4].

4.6 Results

For testing our model we use the screw and material parameters in Table 4.1. We compare our model to the model in [5] that does not include heat and the model in [4] which includes heat generation.

4.6.1 Low RPM and Near Instantaneous Heat Diffusion

The model in [4] assumes instantaneous heat diffusion and uniform screw temperature. Our model loosens these assumptions by making heat diffusion time dependent which makes insertion speed an important

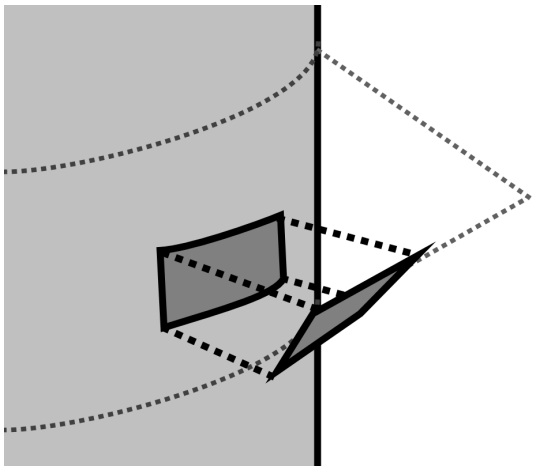

Figure 4.7: A portion of the true heat generating surface being projected onto our cylinder.

variable in the model. As the RPM approaches zero, the heat in the screw will have more time to diffuse during insertion so we would expect our model would converge to the model in [4].

As can be seen in Figure 4.8, our model with a low insertion speed of 5 RPM has a much higher drive torque than the model of [4]. This difference can be attributed to a number of issues. As discussed in Section 4.5.3, we are generating less heat than the model described in [4]. One way to possibly overcome this difference is to change the rate at which heat is generated in our model. In a screw, the friction is not being generating at an outward radius of $D_r/2$ as we use in (4.13); a better approximation would be

$$\frac{\partial \mathscr{T}}{\partial n} = -\frac{\mu_1 \sigma_{uts} \pi \omega \frac{D_h + D_s}{2}}{K \cos \theta'} \tag{4.27}$$

since the average outward radius of a point of the thread generating heat is $\frac{D_h+D_s}{2}$. Note, we keep the radius of the model cylinder at $D_r/2$; only the rate of heat generation is changed. The results of using this new radius can be seen in Figure 4.9. Using the larger radius $\frac{D_h+D_s}{2}$ we generate more heat than if we were to use $D_r/2$ and thus the required torque is lowered. However, it is clear that we have still not accounted for all of the differences between our model and the model in [4]. Section 4.5.3 describes that the area could be one of the reasons for this drastic difference, as well as this the work done in Section 4.5.1 could be a source of part of the difference since we do not generate heat at a constant rate.

There are several other interesting results from Figure 4.9. In the figure, the change in radius affected the screw being inserted at 900 RPM significantly more than the screw being inserted at 5 RPM. This is most likely because the heat being generated has less time to diffuse into the screw so it remains closer to the surface and thus has more of an impact on insertion. The curve generated by [4] has a linear decrease in torque after breakthrough but before tightening, while our curve does not. This can be attributed to several factors. In the model of [4], after breakthrough, heat is generated at a constant rate, while in our model heat is not generated at a constant rate as we explain in Section 4.5.1. Also some of the heat on the surface of the screw may be diffusing into the screw, which would affect our model but not the model of 4.5.1.

Table 4.1: Parameters for Test 1 [ABS]

Screw Properties		Plate Properties	
Major Diameter D_s	3.42 mm	Tap Hole Diameter	2.5 mm
Root Diameter D_r	2.49 mm	Near Hole Diameter	0.0 mm
Screw Head Diameter	6.52 mm	Draft Angle	0
Point Diameter	0.00 mm	Near Plate Thickness	0
Pitch	1.19 mm	Tap Plate Thickness	4.46 mm
Length	9.67 mm	Elastic Modulus	2.35 GPa
Taper Length	2.94 mm	Friction Coef. (Tap) μ	0.19
Trail Angle	30 deg.	Yield Strength	45 MPa
Lead Angle	30 deg.	Tensile Strength σ_{uts}	45 MPa
Engagement Rotation	0 deg.	Compressive Strength	45 MPa
Thermal conductivity	51.9 W/m·K	Thermal conductivity	0.128 W/m·K
Density	7.8 g/cc	Density	1.02 g/cc
Specific heat capacity	0.486 J/g·K	Specific heat capacity	1.96 J/g·K
Initial Temperature	20° C		

4.6.2 Effects of RPM

Before creating the model, we hypothesized that an increase in RPM would decrease the amount of torque required to insert the screw. The reasoning for this hypothesis was that if the screw was inserted quickly there would be less time for the heat generated by friction to diffuse into the center of the screw and the air. Since the heat would stay near the surface of the screw it would have more of an affect on the ultimate tensile strength and thus decrease the required torque. Figure 4.10 shows the torque curves generated by different insertion speeds. It appears that our hypothesis was correct; a higher insertion speed lowered the drive torque of the screw. The speed of screw insertion did not seem to have a drastic effect on the torque curve, although further experimental evidence is needed to determine if this is accurate.

Figure 4.11 shows the temperature of the surfaces of screw shafts at seating. Notice that at higher insertion speeds the change in temperature along the surface is more abrupt. This is because there is less time for the heat to diffuse from the heat generating thread to the rest of the screw surface. Surprisingly the screw does not seem significantly warmer at the time of seating when the screw is inserted at a high RPM. We attribute this to the work done in Section 4.5.1.

4.6.3 Conclusion

When testing our model it became clear that a higher screw insertion speed lowered the drive torque of the screw. This decrease was a relatively small amount compared to the drive torque itself. This decrease is promising, however further research should be done to compare our results with experimental data generated by BOSE.

When we compared the torque curve generated with out heat model to the ones generated using the work of Miller et al. we found that although they had a similar shape, our model required more torque to overcome friction. It is likely that the higher required torque is due to the reasons discussed in Section 4.5.3, however more research needs to be done before we can be certain.

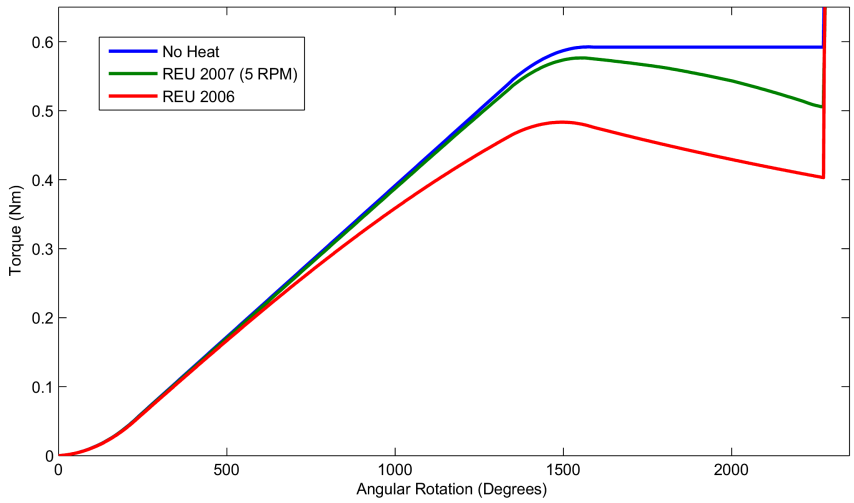

Figure 4.8: A comparison of our model of screw insertion using near instantaneous heat distribution with the model of [4] and the heatless model.

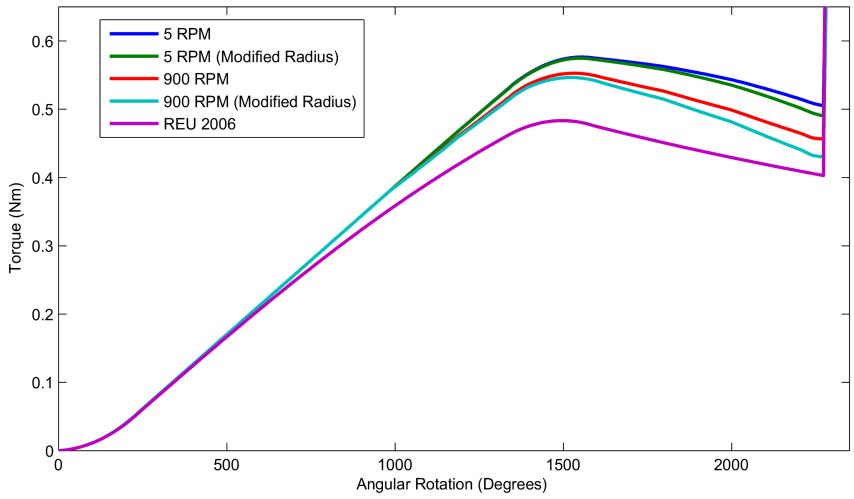

Figure 4.9: A comparison of our model of screw insertion using near instantaneous heat distribution with the model of [4] and the heatless model.

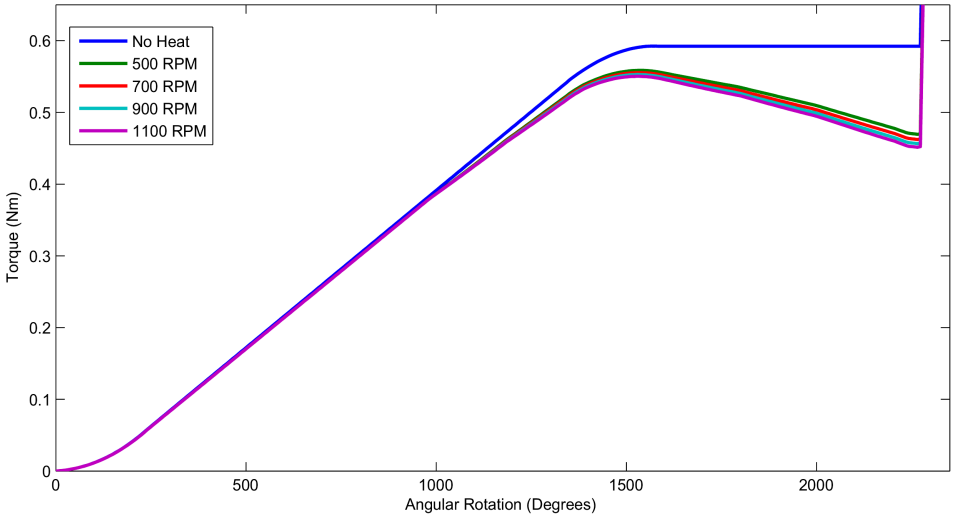

Figure 4.10: A comparison of the torque curves generated with different insertion speeds.

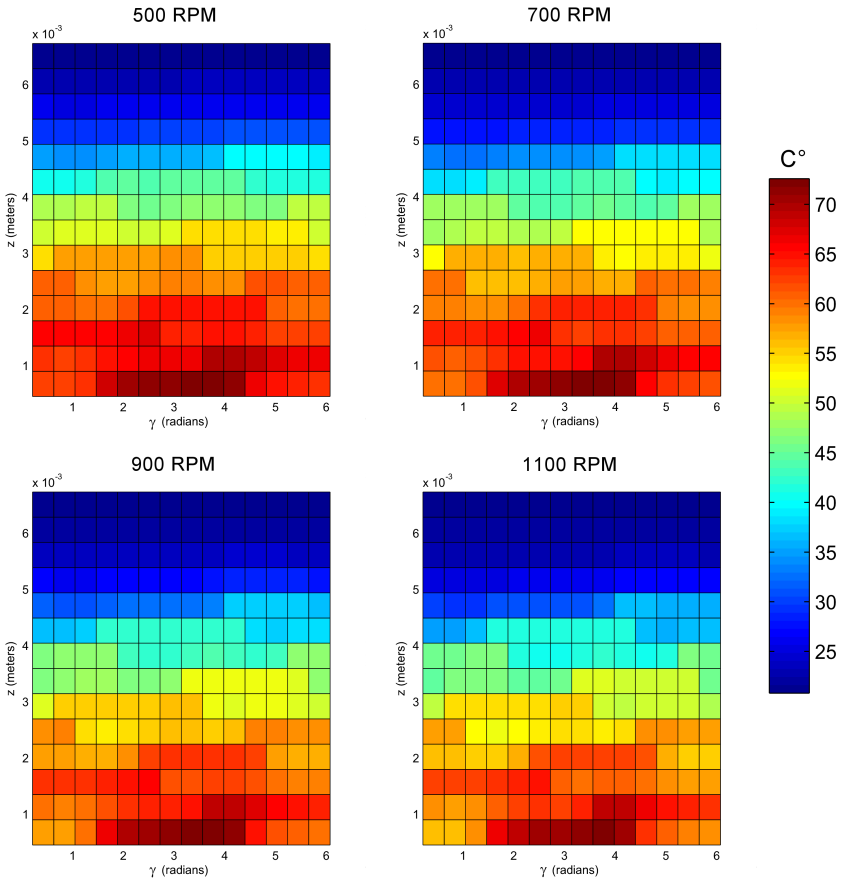

Figure 4.11: The effect of insertion speed on screw surface temperature at seating

Bibliography

[1] John H. Bickford, An Introduction to the Design and Behavior of Bolted Joints, Marcel Dekker, Inc. New York, New York, 1990.

[2] Effect of Temperature and Other Factors on Plastics, William Andrew Publishing/Plastics Design Library, 1990. Online version available at: http://www.knovel.com/knovel2/Toc.jsp?BookID=375&VerticalID=0

[3] Franklin Jones, Henry Ryffel, Christopher McCauley, Robert Green, and Ricardo Heald. Machinery's Handbook Guide. 27th ed. New York, NY: Industrial Press Inc., 2004.

[4] J. Miller, A. Shved, and L. Tang, Model for Self-tapping Screw Tightening Process and Heat Generation, REU paper at WPI, Worcester, MA, 2006.

[5] A. Leo, S. Manivanna, and J. Potter, Mathematical Modeling of the Torque for Screw Insertion Process, MQP paper at WPI, Worcester, MA, 2006.

[6] R.L. Norton, Machine Design: An Integrated Approach, Prentice-Hall, Upper Saddle River, NJ, 1998.

[7] E. Rabinowicz, Friction and Wear of Materials, John Wiley & Sons, Inc., New York, 1965.

[8] L. Seneviratne, F. Negmoh, S. Earles, and K. Althoefer, Theoretical modelling of the self-tapping screw fastening process, Proceedings of IMechE, Part C, Journal of Mechanical Engineering Science, 215 pp.135-154, 2001.

[9] Torque Tightening. Bolt Science. 2007. Bolt Science Limited. 3 Jul 2007 http://www.boltscience.com/pages/faq.htm.